



RESEARCH LETTER

10.1002/2014GL061541

Key Points:

- Revised estimate and uncertainty of post-2000 volcanic forcing and temperature
- Significant unaccounted volcanic aerosol between the tropopause and 15 km
- Novel use of AERONET to derive total stratospheric aerosol optical depth

Supporting Information:

- Readme
- Text S1, Tables S1 and S2, and Figures S1–S5

Correspondence to:

D. A. Ridley,
daridley@mit.edu

Citation:

Ridley, D. A., et al. (2014), Total volcanic stratospheric aerosol optical depths and implications for global climate change, *Geophys. Res. Lett.*, *41*, doi:10.1002/2014GL061541.

Received 14 AUG 2014

Accepted 29 OCT 2014

Accepted article online 31 OCT 2014

Total volcanic stratospheric aerosol optical depths and implications for global climate change

D. A. Ridley¹, S. Solomon², J. E. Barnes³, V. D. Burlakov⁴, T. Deshler⁵, S. I. Dolgii⁴, A. B. Herber⁶, T. Nagai⁷, R. R. Neely III⁸, A. V. Nevzorov⁴, C. Ritter⁹, T. Sakai⁷, B. D. Santer¹⁰, M. Sato¹¹, A. Schmidt¹², O. Uchino⁷, and J. P. Vernier^{13,14}

¹Department of Civil and Environmental Engineering, Massachusetts Institute of Technology, Cambridge, Massachusetts, USA, ²Department of Earth, Atmospheric, and Planetary Science, Massachusetts Institute of Technology, Cambridge, Massachusetts, USA, ³Mauna Loa Observatory, NOAA, Hilo, Hawaii, USA, ⁴V.E. Zuev Institute of Atmospheric Optics, Siberian Branch, Russian Academy of Sciences, Tomsk, Russia, ⁵Department of Atmospheric Sciences, University of Wyoming, Laramie, Wyoming, USA, ⁶Alfred Wegener Institute, Helmholtz Centre for Polar and Marine Research, Bremerhaven, Germany, ⁷Meteorological Research Institute, Tsukuba, Ibaraki, Japan, ⁸Advanced Study Program, National Center for Atmospheric Research, Boulder, Colorado, USA, ⁹Alfred Wegener Institute, Helmholtz Centre for Polar and Marine Research, Potsdam, Germany, ¹⁰Program for Climate Model Diagnosis and Intercomparison, Lawrence Livermore National Laboratory, Livermore, California, USA, ¹¹The Earth Institute, Columbia University, New York, New York, USA, ¹²School of Earth and Environment, University of Leeds, Leeds, UK, ¹³Science Systems and Applications, Inc., Hampton, Virginia, USA, ¹⁴NASA Langley Research Center, Hampton, Virginia, USA

Abstract Understanding the cooling effect of recent volcanoes is of particular interest in the context of the post-2000 slowing of the rate of global warming. Satellite observations of aerosol optical depth above 15 km have demonstrated that small-magnitude volcanic eruptions substantially perturb incoming solar radiation. Here we use lidar, Aerosol Robotic Network, and balloon-borne observations to provide evidence that currently available satellite databases neglect substantial amounts of volcanic aerosol between the tropopause and 15 km at middle to high latitudes and therefore underestimate total radiative forcing resulting from the recent eruptions. Incorporating these estimates into a simple climate model, we determine the global volcanic aerosol forcing since 2000 to be $-0.19 \pm 0.09 \text{ Wm}^{-2}$. This translates into an estimated global cooling of 0.05 to 0.12°C. We conclude that recent volcanic events are responsible for more post-2000 cooling than is implied by satellite databases that neglect volcanic aerosol effects below 15 km.

1. Introduction

Over about the past 15 years, globally averaged surface temperatures have increased more slowly than during the two previous decades ($\approx 1980\text{--}2000$), a phenomenon sometimes referred to as the “hiatus” or “pause” in global warming. Suggested mechanisms that may contribute to this behavior include (but are not limited to) increased heat uptake by the oceans, reduced solar output, and recent volcanic eruptions (see the brief review by Schmidt *et al.* [2014, and references therein]).

It has often been assumed that only very explosive volcanic eruptions have pronounced effects on stratospheric aerosol optical depth (SAOD) and that since Mount Pinatubo in 1991, no eruptions have contributed noticeably to stratospheric aerosol content. However, observations since about 2005 revealed significant increases in SAOD linked to a series of smaller eruptions [Vernier *et al.*, 2011; Bourassa *et al.*, 2012], with potentially important cooling effects on global climate [Solomon *et al.*, 2011; Fyfe *et al.*, 2013; Haywood *et al.*, 2014].

Available satellite observations of SAOD typically consider aerosol extinction only above 15 km to reduce potential contamination by clouds. However, a portion of the lower stratosphere generally resides below this altitude at middle and high latitudes, where the tropopause is frequently found at 10 km or lower. Here we present evidence for a significant contribution to SAOD from the lowermost stratosphere region. Based on observations from lidar retrievals, balloon-borne aerosol sondes, ground-based Aerosol Robotic Network (AERONET) Sun photometers, and satellite data, we estimate increases in global total SAOD since 2000, together with associated uncertainties. The resulting total estimated volcanic aerosol forcing averaged over the period 2000–2013 is found to be $-0.19 \pm 0.09 \text{ Wm}^{-2}$, up to 80% larger than the estimate of Solomon *et al.* [2011].

2. Observational Data Sets

In this study we make use of SAOD retrievals from multiple observing systems: four lidars measuring backscatter at 532 nm, a balloon-borne particle counter (aerosol sonde), Sun photometers in the Aerosol Robotic Network (AERONET), and two satellite data sets. The polarization lidar at Tsukuba (36.1°N, 140.1°E) provides backscatter integrals both above the tropopause and above 15 km [Uchino *et al.*, 2012]. The lidar based at Tomsk (56.5°N, 85.0°E) makes similar measurements of integrated backscatter both above 12 km and 15 km [Bazhenov *et al.*, 2011]. At Ny Ålesund (78.9°N, 11.9°W), lidar backscatter was obtained both above 10 km and 15 km [Hoffmann *et al.*, 2009], while at Mauna Loa (19.5°N, 155.6°W), backscatter integrated above the tropopause (typically at 15–16 km) has been monitored since 2000 [Hofmann *et al.*, 2009]. The Ny Ålesund and Tomsk data presented here are integrations from fixed altitudes of 10 km and 12 km, rather than at the tropopause; for simplicity, however, throughout the analysis, we will refer to the lidar retrievals as either “above tropopause” or “above 15 km.” All of these integrated 532 nm backscatter measurements were converted to SAOD using a lidar ratio (integrated extinction/backscatter) of 50 [see Jäger and Deshler, 2002, 2003]. The Laramie aerosol sondes have measured detailed particle size distributions since 2000 and were used to confirm that a lidar extinction to backscatter ratio of 50 is still appropriate for the stratosphere; this was found to be the case within an uncertainty of 10–20%.

The Laramie data extend from the surface to typically 30 km [Deshler *et al.*, 2003]. SAOD is computed above 15 km and above the tropopause through integrations of 532 nm extinction calculated from the profile of size distribution measurements, using a refractive index of 1.45—0i for stratospheric sulfate. Days with tropopause heights above 15 km are not included in the comparisons presented here (14% of the observations).

Satellite retrievals of SAOD are presented below from two data sets, both of which integrate aerosol loads above 15 km altitude. Sato *et al.* [1993], updated on the NASA Goddard Institute for Space Studies website, and hereafter referred to as Sato *et al.*, have produced a long-term (1850 to present) reconstruction from a variety of observations, relying exclusively on Optical Spectrograph and InfraRed Imager System satellite measurements [Bourassa *et al.*, 2008] since 2001. We also show an updated version of the merged SAOD data set developed by Vernier *et al.* [2011, hereafter referred to as Vernier *et al.*], which extends from 50°S to 50°N and incorporates satellite data from multiple platforms (Stratospheric Aerosol and Gas Experiment (SAGE) II between October 1984 and August 2005, SAGE III from February 2002 until the end of 2005, and Global Ozone Monitoring by Occultation of Stars from 2006 onward).

3. Detecting Volcanic Aerosol With AERONET Observations

To provide an independent estimate of the total column SAOD, we make use of observations from AERONET Sun photometers deployed at ground sites worldwide to measure total aerosol optical depth. The widespread coverage of these stations, which span a wide range of elevations, is key to a global analysis. These measurements are often used as calibration for satellite retrievals and are considered to have an aerosol optical depth retrieval error of <0.01 at wavelengths 440 nm and greater [Holben *et al.*, 1998]. While the majority of the aerosol detected is often tropospheric, we will show that the quality of the retrieval, availability of daily data, and the large number of stations providing information make estimation of SAOD feasible. Because the measured SAOD at certain locations and times may be close to the retrieval accuracy of the instrument, we employ a range of methods to ensure data quality and robust results (see supporting information).

Solomon *et al.* [2011] compared tropical satellite, lidar, and surface-based optical depth data for 21st century volcanic eruptions. They showed that surface-based optical depth observations from the clearest days of the year at Mauna Loa were dominated by stratospheric signals following volcanic eruptions and agreed well with other observation methods. Here we perform a similar analysis at a variety of stations using AERONET data. To ensure that AERONET measurements can provide a reliable estimate of volcanic SAOD, we demonstrate that the timing of the increase in SAOD is significantly correlated with volcanic eruptions and that the ability to detect volcanic signatures is not significantly affected by station location and sampling periods. We also compare AERONET data to lidar observations.

We briefly describe the approach taken to derive stratospheric information from AERONET data, see supporting information for a detailed discussion. At each station, the minimum AOD at 500 nm (AOD_{\min}) observed on the five cleanest days within a year is averaged. The data are quality checked by ensuring that

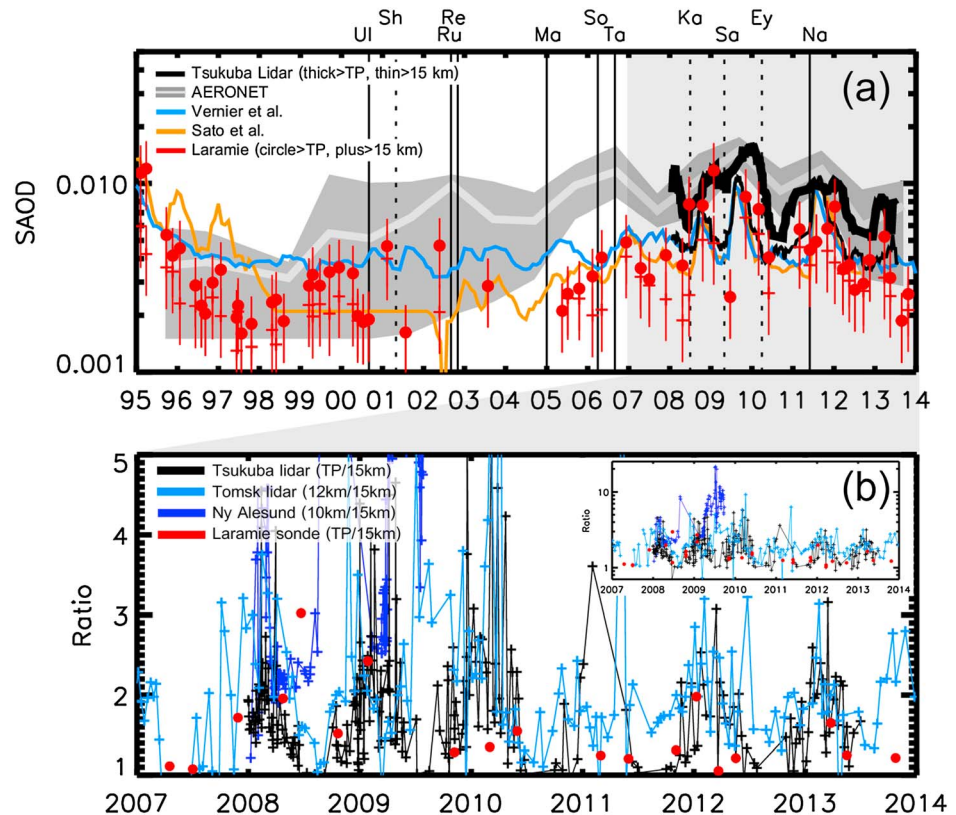


Figure 1. (a) The SAOD time series for the period 1995–2013 for satellite data from Vernier et al. (blue), Sato et al. (orange), AERONET mean, averaged from 30–45°N, (white) with 25th to 75th percentile uncertainty (grey shading), Tsukuba lidar retrievals (36.1°N, 140.1°E) above the tropopause (thick black line) and 15 km (thin black line), and aerosol sonde measurements at Laramie (41°N) above the tropopause (red dots) and 15 km (red crosses). Potentially important equatorial (solid lines) and middle to high latitude (dashed lines) volcanic eruptions are shown for Ulawun, Shiveluch, Ruag, Reventador, Manam, Soufrière Hills, Tavurvur, Kasatochi, Sarychev, Eyjafjallajökull, and Nabro. (b) Ratio of integrated optical depth above the tropopause to that above 15 km from three different lidars and from the in situ observations. The inset contains the same data on a log scale to indicate the ratios greater than 5 that are cropped for clarity on Figure 1a.

these minimum AOD observations are within a factor of 2 of one another. Any values that fail these criteria are discarded to remove bias by potential individual measurement errors (this rarely occurs). The averaging removes transient tropospheric features, such as anthropogenic pollution episodes and biomass burning events, but should capture persistent enhancements in the stratospheric aerosol observed after eruptions. Systematic enhancements in AOD_{min} are evident following the series of recent eruptions (Figures S1 and S3 in the supporting information). Two different Monte Carlo tests were used to check the robustness of the link of these apparent AERONET enhancements in AOD_{min} to the eruptions: first, by randomizing the timing of the 11 larger eruptions since 2000 and second, by randomizing the years of the AERONET data. These tests showed that the increases in AERONET-based AOD_{min} measurements following the 11 selected eruptions are significant at the 10% level or better (see supporting information).

We find that the lowest AOD measured at each AERONET station is strongly dependent on station elevation, which is key to our analysis. Stations closer to sea level do not sample conditions as pristine as those at higher elevations, leading to a robust relationship between the logarithm of a station's elevation and the minimum AOD at that station. Using this relationship, we obtain the AOD as the measured enhancement above the clean background SAOD and tropospheric AOD for the time series (see Figure S2 in the supporting information); a clean background stratospheric AOD of 0.0015 is then added to each data point to obtain the total SAOD. The estimated SAOD is averaged across all available AERONET stations within four latitude bands: 30°S–30°N (8 stations), 30°N–45°N (22 stations), 45°N–60°N (6 stations), and 60°N–90°N (8 stations). A sampling uncertainty range for the AERONET estimate of SAOD is developed by creating ensembles of three

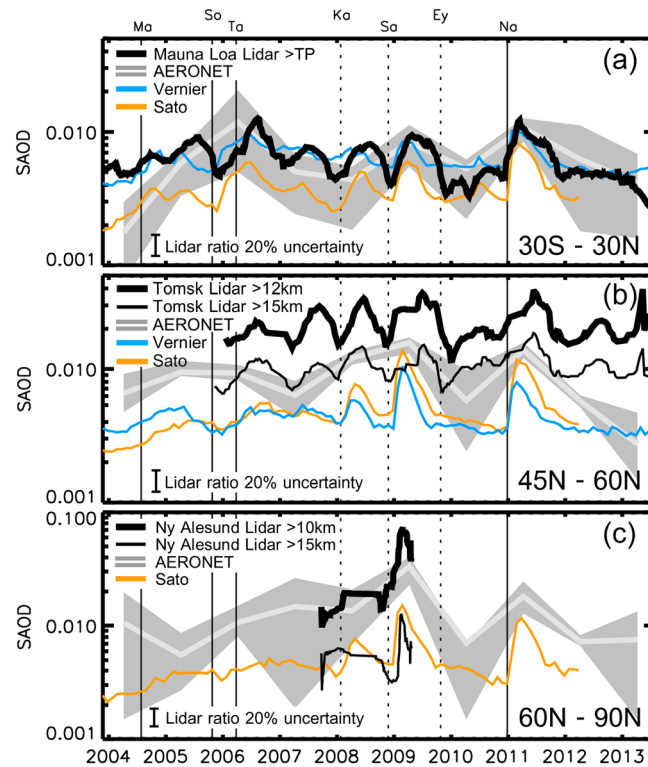


Figure 2. SAOD time series for the period 2004–2013 between (a) 30°S–30°N, (b) 45°N–60°N, and (c) 60°N–90°N. As in Figure 1, satellite data from Vernier et al. (blue), Sato et al. (orange), and the AERONET mean (light grey) as well as the 25th to 75th percentile uncertainty (grey shading). Lidar retrievals at 15 km (thin black lines) and 10 km/12 km (thick black lines) are shown. At Mauna Loa, the tropopause is at 15–16 km, so only a single line is shown. The solid and dashed vertical lines indicate the tropical and higher-latitude eruptions, respectively.

The ratio of the lidar data above the tropopause to that above 15 km (Figure 1b) demonstrates the key role of the lowermost stratosphere for total SAOD. The Laramie balloon data are sparse and are generally lower in absolute values than the lidar but display ratios of the SAOD integrated above the tropopause and above 15 km that are very similar to those measured by the Tsukuba lidar, again showing the importance of the contribution from the lower stratosphere. Based on the Tsukuba lidar and aerosol sonde observations, an average of 28–39% of the optical depth observed above the tropopause resides below 15 km. At times, the contribution of this region to total SAOD is as large as 66–82%. We note, however, that not all of the SAOD contribution below 15 km can be attributed to volcanic aerosol, especially in the winter and spring months when the tropopause is lowest. This is evident from the seasonal variations in SAOD.

The AERONET SAOD values are generally larger than those of the satellite data sets but are in good agreement with the lidar SAOD above the tropopause (see Figure S4 in the supporting information). Prior to 2007, the mean AERONET SAOD often exceeds the satellite SAOD by over a factor of 2, although the uncertainty range generally encompasses the Vernier data. The fact that the aerosol sonde SAOD shows very similar enhancements following eruptions to that found at Tsukuba, but is generally lower than the satellite and lidar data, adds to the uncertainty in the absolute values of SAOD.

Figure 1b also presents ratios between the SAOD integrated above the tropopause and above 15 km from two higher-latitude lidar stations, Tomsk and Ny Ålesund. It provides further evidence that at certain locations, the region below 15 km contributes markedly to total SAOD, particularly in the winter season or immediately following nearby eruptions (e.g., Ny Ålesund in summer 2009, which directly sampled the Sarychev Peak plume). The observational study by Jégou et al. [2013] independently confirms the importance of volcanic aerosol below 15 km following Sarychev.

randomly selected stations in each latitude band, from which we determine the mean annual SAOD. The 25th to 75th percentiles of the ensemble means are considered the uncertainty range, thereby minimizing the chance of the AERONET SAOD estimate being dominated by a single station.

4. Multi-Instrument Estimates of SAOD Above and Below 15 km

Figure 1a shows the observed SAOD time series for 1995–2013 obtained from the annual averages of AERONET data from 30 to 45°N and compared with satellite data (Vernier et al.; Sato et al.), the lidar at Tsukuba (36°N), and aerosol sondes from Laramie, WY (41°N). Because of strong zonal winds, we assume that stratospheric aerosol at a given latitude becomes well mixed within a few weeks or so, allowing meaningful comparisons within a latitude band. The satellite and Tsukuba lidar data integrated above 15 km agree on the magnitude and timing of SAOD enhancements associated with known eruptions. However, at this latitude, the lidar reveals substantially larger SAOD when integrated above the tropopause.

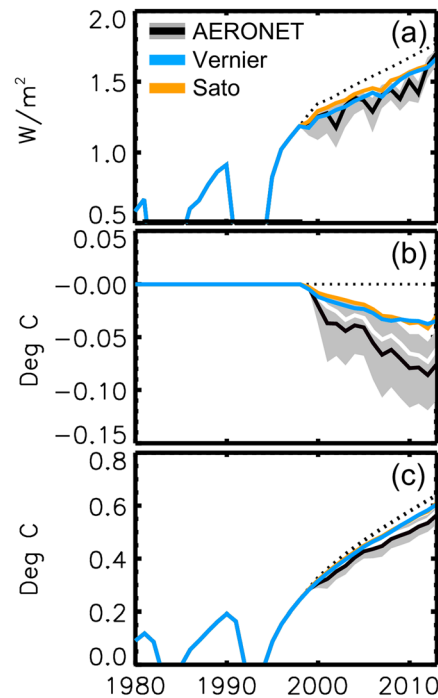


Figure 3. (a) Estimated global mean radiative forcing is shown for data sets from Sato et al. (orange), Vernier et al. (blue), and AERONET mean (black) with 25th to 75th percentile ranges (grey). The dotted line indicates the baseline model used in many climate model studies to date, which includes no stratospheric aerosol changes after 2000. (b) The temperature anomaly, relative to the baseline model, including the AERONET mean (black), median (white), and 25th to 75th percentile ranges (grey); Vernier et al. (blue); and Sato et al. (orange) forcing computed for each data set. (c) The total global temperature change predicted by the Bern 2.5cc EMIC in response to combined anthropogenic and natural forcing, including the reduced warming when considering the stratospheric aerosol forcing from the three data sets.

Figure 2 displays the comparisons between the satellite-inferred SAOD at a range of latitude bands and corresponding SAOD estimates from the Mauna Loa, Tomsk, and Ny Ålesund lidars between 2004 and 2013. Agreement between lidar, AERONET, and the Vernier et al. and Sato et al. data sets is excellent in the tropics (30°S–30°N; Figure 2a), where the tropopause is close to 15 km. Aerosols from tropical eruptions will, however, be transported downward and poleward over time, so that the aerosol column burden above the tropopause at the middle and high latitudes will be larger than that above 15 km, especially in winter (just as occurs for column ozone). At subpolar midlatitudes (45–60°N; Figure 2b), the Tomsk lidar retrievals also suggest that a substantial amount of the total stratospheric optical depth (about 50% on average) comes from the region between 12 km and 15 km. However, unlike the other locations, the Tomsk lidar SAOD above 15 km is generally 0.005 greater than the satellite data sets during clean periods, and the integral above 12 km is often 0.01 higher than the AERONET mean. Because the altitude is fixed at 12 km, rather than tracking the tropopause height, there is potential for tropospheric aerosol to be present in this measurement. At high latitudes (60–90°N; Figure 2c), the Ny Ålesund lidar indicates that 72% of the SAOD resides between 10 km and 15 km between 2008 and 2010. After the Sarychev Peak (48°N) eruption, almost all the SAOD is present below 15 km. Therefore, while the Sato data set is in good agreement with lidar retrievals at Ny Ålesund above 15 km, the Sato data set does not account for the vast majority of the SAOD at this latitude. Although the lidar data are limited, the annual AERONET SAOD appears to represent well the SAOD before and after the Sarychev Peak eruption when compared with the lidar above 10 km. Our study does not quantify all of the many possible sources of structural uncertainty. While it is clear that the Sato et al. and Vernier et al. data sets neglect important contributions from the lowermost stratosphere below 15 km that are evident in both aerosol sonde and lidar data, the former also suggest that uncertainties in optical properties are important and the lidar data could be biased high.

5. SAOD Radiative Forcing and Global Mean Climate Response

Figure 3 presents estimates of the effect of the SAOD (from Vernier et al., Sato et al., and AERONET, with the previously described uncertainty bound on the latter) on radiative forcing and global-mean temperature change based on the Bern 2.5cc Earth Model of Intermediate Complexity (EMIC) [Plattner et al., 2008], which was run in the same configuration used by Solomon et al. [2011]. The SAOD from each AERONET latitude band is weighted by the band surface area and combined to produce a global average, and this is converted to a forcing using a scaling factor of -25 Wm^{-2} , following Solomon et al. [2011]. Since most AERONET stations are located north of 30°S, we obtain a conservative estimate of global-mean SAOD by making the simplifying assumption that the SAOD between 30°S and 90°S is the same as in the tropics. The global-mean SAOD is assumed to be suitable approximation for an EMIC. The Vernier et al. data set is only available equatorward of 50°N and 50°S; we therefore assume that SAOD poleward of 50° is the same as at 50°. AERONET data are limited prior to 2000; therefore, we only introduce the SAOD forcing from each data set in 1999.

The AERONET SAOD produces a mean global radiative forcing of $-0.19 \pm 0.09 \text{ Wm}^{-2}$ between 2000 and 2013 (Figure 3a). Over the same period, the AERONET forcing results in a global temperature reduction ranging

from -0.05°C to -0.12°C , with peak reductions in 2012. With forcings inferred from the Vernier et al. and Sato et al. data sets, temperature changes are smaller (-0.04°C in both cases, see Figures 3b and 3c). Some volcanic aerosol enhancements are expected in the upper troposphere and would be captured by AERONET; on the other hand, tropospheric pollution could lead to a high bias in AERONET despite the approach taken to minimize these effects. Figure 3 suggests a larger volcanic contribution to recent global temperature changes than has been inferred from previous work. Clearly, it is desirable to obtain a more reliable quantification of the contribution of this and other forcings (such as changes in solar activity) to the hiatus [Schmidt et al., 2014] and to reduce uncertainties in observational estimates of the decadal rate of change of global mean temperature [Cowtan and Way, 2014].

6. Discussion

Satellite observations have shown that volcanic eruptions since 2000 introduced aerosol into the stratosphere, and this represents a forcing overlooked in climate models until very recently. The climate model simulations evaluated in the fifth assessment report of the *Intergovernmental Panel on Climate Change* [2014] generally assumed zero stratospheric aerosol after about 2000 and hence neglect any cooling effect of recent volcanoes [see Solomon et al., 2011, Figure 3]. We find that satellite-based SAOD data sets generally agree well with SAOD inferred from lidar measurements above 15 km; however, they do not capture the full magnitude of the SAOD signal above the tropopause. Lidar and balloon-borne observations indicate that aerosol loading between the tropopause and 15 km contributes roughly 30 to 70% of the total SAOD and this percentage can increase further immediately following eruptions. We have shown that AERONET Sun photometers are capable of detecting SAOD sufficiently well to identify enhancements following volcanic eruptions, albeit with large quantitative uncertainties. The magnitude and interannual variability of the AERONET ensemble mean are in good agreement with many independent ground-based lidar observations integrated above the tropopause. The resulting post-2000 global forcing from AERONET data is $-0.19 \pm 0.09 \text{ Wm}^{-2}$, suggesting that the global mean volcanic aerosol forcing could be substantially larger than that used in previous studies.

The SAOD below 15 km may help to explain certain aspects of the sensitivity of lower tropospheric temperature (TLT) to SAOD found by Santer et al. [2014]. They showed that decreases in TLT are negatively correlated with enhancements in SAOD following eruptions; however, the magnitude of the TLT fluctuations (and the high statistical significance of the correlations between Vernier et al. SAOD and TLT) implied a larger TLT response to recent volcanic eruptions than would be expected based solely on the SAOD data above 15 km. Including the substantial “below 15 km” contributions to volcanically induced SAOD signals found in the present study will lead to a more realistic sensitivity of TLT to SAOD, further strengthening the case that “smaller” eruptions have substantially influenced tropospheric temperature in the past decade.

Finally, the SAOD above 15 km most noticeably underestimates the total SAOD at high latitudes following an eruption, particularly a high-latitude eruption. The polar regions account for less than 15% of the global surface area; therefore, while these regions do not contribute greatly to the global forcing, the regional forcing can be markedly affected, for example following high-latitude eruptions such as Sarychev Peak. Further investigation of the regional and global impact of stratospheric aerosol in the current generation of climate models should account for the observational uncertainties in SAOD discussed here. Such studies will help to elucidate the contribution of volcanic aerosol to the warming hiatus.

Acknowledgments

The Laramie in situ aerosol measurements have been supported primarily by the National Science Foundation, with the current measurements funded under grant 1011827. Measurements at Tomsk were supported in part by the Ministry of Science and Education of the Russian Federation (agreements 14.604.21.0046 and 14.604.21.0100) and the Russian Science Foundation (agreement 14-27-00022). The authors would like to thank the PIs of AERONET stations used in this study, the data from which can be obtained at <http://aeronet.gsfc.nasa.gov>.

The Editor thanks two anonymous reviewers for their assistance in evaluating this paper.

References

- Bazhenov, O. E., V. D. Burlakov, S. I. Dolgii, and A. V. Nevzorov (2011), Lidar observations of the stratosphere aerosol disturbances over Tomsk (56.5°N ; 85.0°E) in period of volcanic activity of 2006–2010, *Opt. Atmosf Okeana*, 24(12), 1031–1040.
- Bourassa, A. E., D. A. Degenstein, and E. J. Llewellyn (2008), Retrieval of stratospheric aerosol size information from OSIRIS limb scattered sunlight spectra, *Atmos. Chem. Phys.*, 8(21), 6375–6380, doi:10.5194/acp-8-6375-2008.
- Bourassa, A. E., A. Robock, W. J. Randel, T. Deshler, L. A. Rieger, N. D. Lloyd, E. J. Llewellyn, and D. A. Degenstein (2012), Large volcanic aerosol load in the stratosphere linked to asian monsoon transport, *Science*, 337(6090), 78–81, doi:10.1126/science.1219371.
- Cowtan, K., and R. G. Way (2014), Coverage bias in the HadCRUT4 temperature series and its impact on recent temperature trends, *Q. J. R. Meteorol. Soc.*, 140(683), 1935–1944, doi:10.1002/qj.2297.
- Deshler, T., M. E. Hergiv, D. J. Hofmann, J. M. Rosen, and J. B. Liley (2003), Thirty years of in situ stratospheric aerosol size distribution measurements from Laramie, Wyoming (41°N), using balloon-borne instruments, *J. Geophys. Res.*, 108(D5), 4167, doi:10.1029/2002JD002514.
- Fyfe, J. C., K. von Salzen, J. N. S. Cole, N. P. Gillett, and J.-P. Vernier (2013), Surface response to stratospheric aerosol changes in a coupled atmosphere–ocean model, *Geophys. Res. Lett.*, 40, 584–588, doi:10.1002/grl.50156.

- Haywood, J. M., A. Jones, and G. S. Jones (2014), The impact of volcanic eruptions in the period 2000–2013 on global mean temperature trends evaluated in the HadGEM2-ES climate model, *Atmos. Sci. Lett.*, *15*(2), 92–96, doi:10.1002/asl2.471.
- Hoffmann, A., C. Ritter, M. Stock, M. Shiobara, A. Lampert, M. Maturilli, T. Orgis, R. Neuber, and A. Herber (2009), Ground-based lidar measurements from Ny-Ålesund during ASTAR 2007, *Atmos. Chem. Phys.*, *9*(22), 9059–9081, doi:10.5194/acp-9-9059-2009.
- Hofmann, D., J. Barnes, M. O'Neill, M. Trudeau, and R. Neely (2009), Increase in background stratospheric aerosol observed with lidar at Mauna Loa Observatory and Boulder, Colorado, *Geophys. Res. Lett.*, *36*, L15808, doi:10.1029/2009GL039008.
- Holben, B. N., et al. (1998), AERONET—A federated instrument network and data archive for aerosol characterization, *Remote Sens. Environ.*, *66*(1), 1–16, doi:10.1016/S0034-4257(98)00031-5.
- Intergovernmental Panel on Climate Change (Ed.) (2014), *Climate Change 2013 – The Physical Science Basis: Working Group I Contribution to the Fifth Assessment Report of the Intergovernmental Panel on Climate Change*, Cambridge Univ. Press, Cambridge.
- Jäger, H., and T. Deshler (2002), Lidar backscatter to extinction, mass and area conversions for stratospheric aerosols based on midlatitude balloonborne size distribution measurements, *Geophys. Res. Lett.*, *29*, 1929, doi:10.1029/2002GL015609.
- Jäger, H., and T. Deshler (2003), Correction to “Lidar backscatter to extinction, mass and area conversions for stratospheric aerosols based on midlatitude balloonborne size distribution measurements”, *Geophys. Res. Lett.*, *30*(7), 1382, doi:10.1029/2003GL017189.
- Jégou, F., et al. (2013), Stratospheric aerosols from the Sarychev volcano eruption in the 2009 Arctic summer, *Atmos. Chem. Phys.*, *13*(13), 6533–6552, doi:10.5194/acp-13-6533-2013.
- Plattner, G.-K., et al. (2008), Long-term climate commitments projected with climate–carbon cycle models, *J. Clim.*, *21*(12), 2721–2751, doi:10.1175/2007JCLI1905.1.
- Santer, B. D., et al. (2014), Volcanic contribution to decadal changes in tropospheric temperature, *Nat. Geosci.*, *7*(3), 185–189, doi:10.1038/ngeo2098.
- Sato, M., J. E. Hansen, M. P. McCormick, and J. B. Pollack (1993), Stratospheric aerosol optical depths, 1850–1990, *J. Geophys. Res.*, *98*(D12), 22,987–22,994, doi:10.1029/93JD02553.
- Schmidt, G. A., D. T. Shindell, and K. Tsigaridis (2014), Reconciling warming trends, *Nat. Geosci.*, *7*(3), 158–160, doi:10.1038/ngeo2105.
- Solomon, S., J. S. Daniel, R. R. Neely, J.-P. Vernier, E. G. Dutton, and L. W. Thomason (2011), The persistently variable “Background” stratospheric aerosol layer and global climate change, *Science*, *333*(6044), 866–870, doi:10.1126/science.1206027.
- Uchino, O., et al. (2012), On recent (2008–2012) stratospheric aerosols observed by lidar over Japan, *Atmos. Chem. Phys.*, *12*(24), 11,975–11,984, doi:10.5194/acp-12-11975-2012.
- Vernier, J.-P., et al. (2011), Major influence of tropical volcanic eruptions on the stratospheric aerosol layer during the last decade, *Geophys. Res. Lett.*, *38*, L12807, doi:10.1029/2011GL047563.